

# Washcoating and chemical testing of a commercial Cu/ZnO/Al<sub>2</sub>O<sub>3</sub> catalyst for the methanol synthesis over copper open-cell foams

Andrea Montebelli<sup>a</sup>, Carlo Giorgio Visconti<sup>a</sup>, Gianpiero Groppi<sup>a</sup>, Enrico Tronconi<sup>a,\*</sup>, Stefanie Kohler<sup>b</sup>, Hilde Johnsen Venvik<sup>c</sup>, Rune Myrstad<sup>d</sup>

<sup>a</sup> Politecnico di Milano, Dipartimento di Energia, Laboratorio di Catalisi e Processi Catalitici, Piazza L. da Vinci 32, 20133 Milano, Italy

<sup>b</sup> Total Refining & Chemicals, 2 place Jean Millier—La Défense 6, 92078 Paris La Défense Cedex, France

<sup>c</sup> Norwegian University of Science and Technology, Department of Chemical Engineering, 7491 Trondheim, Norway

<sup>d</sup> SINTEF Materials and Chemistry, 7456 Trondheim, Norway

Received 19 February 2014

Received in revised form 29 April 2014

Accepted 5 May 2014

Available online 14 May 2014

## 1. Introduction

Methanol is (by volume) one of the top 5 chemical commodities shipped around the world each year, being the raw material for the production of a wide range of oxygenated chemicals (e.g. formaldehyde, methyl *tert*-butyl ether) and hydrocarbons (e.g. ethene, propene through the so-called Methanol-To-Olefins (MTO) process) or as substitute for traditional oil-based fuels for internal combustion engines (ICEs) [1–4].

According to the mature and well-developed ICI process (Imperial Chemical Industries, 1966), the low temperature-low pressure methanol synthesis is industrially carried out using H<sub>2</sub>/CO/CO<sub>2</sub>

mixtures and Cu/ZnO/Al<sub>2</sub>O<sub>3</sub> pelletized catalysts in fixed-bed reactors with quench or multi-tubular cooling [2].

For both reactor configurations, process intensification requires the accurate control of the temperature profile in the catalytic bed, in view of maximizing the syngas conversion per pass and extending the catalyst life (i.e. minimizing the number of shut-downs) as well as minimizing the selectivity toward byproducts like dimethyl ether and methyl formate [5,6].

In particular, in commercial Lurgi externally-cooled multi-tubular packed-bed (PB) reactors, the dominant convective heat transfer mechanism requires the adoption of high flow rates to grant acceptable heat transfer coefficients and to properly control the hot-spot in the reactor. This typically implies the use of long (i.e. several meters) tubes, which seriously limits the possibility of developing compact reactor configurations [7].

\* Corresponding author. Tel.: +39 02 2399 3264; fax: +39 02 2399 3318.  
E-mail address: [enrico.tronconi@polimi.it](mailto:enrico.tronconi@polimi.it) (E. Tronconi).

## Nomenclature

$a$	pore diameter of the bare foam [mm]
$d_p$	catalyst particle size [ $\mu\text{m}$ ]
$d_{50}$	catalyst particle median diameter [ $\mu\text{m}$ ]
$d_c$	cell diameter of the bare foam [mm]
$d_{foam}$	open-cell foam diameter [mm]
$d_s$	strut diameter of the bare foam [mm]
$F_i$	molar flow of species $i$ [mol/s]
$GHSV$	gas hourly space velocity [NI/h/kg <sub>cat</sub> ]
$ID$	reactor tube internal diameter [mm]
$L$	reactor tube length [cm]
$L_{foam}$	open-cell foam length [mm]
$M$	syngas stoichiometric number [–] ( $M = x_{H_2} - x_{CO_2}/x_{CO} + x_{CO_2}$ )
$M_{MeOH}^{liq}$	mass of methanol collected in liquid sample [g]
$\dot{M}_{MeOH}^{off-gas}$	methanol mass flow contained in the off gas [g/h]
$MW$	molecular weight [g/mol]
$P$	pressure [bar]
$PD$	foam pore density, expressed in pores per linear inch, [PPI]
$Prod_{MeOH}$	methanol productivity [g/h/g <sub>cat</sub> ]
$Q$	total volumetric flow [Nml/min]
$RT$	room temperature (i.e. 298 K)
$t_{hold}$	holding time [h]
$t_{saml}$	sampling time [h]
$T$	temperature [K]
$T.o.S$	time on stream [d]
$V_{wash}$	washcoat volume [m <sup>3</sup> ]
$V_{foam}$	foam volume [m <sup>3</sup> ]
$V_{struts}$	bare struts volume [m <sup>3</sup> ]
$x_i$	molar fraction of species $i$ [mol/mol]
<b>Greek symbols</b>	
$\delta_{wash}$	washcoat thickness [m <sup>3</sup> <sub>void</sub> /m <sup>3</sup> <sub>react</sub> ]
$\varepsilon$	bare foam void fraction [m <sup>3</sup> <sub>void</sub> /m <sup>3</sup> <sub>react</sub> ]
$\xi$	catalyst/washcoat volumetric fraction [m <sup>3</sup> <sub>cat</sub> /m <sup>3</sup> <sub>react</sub> ]
$\rho_{H_2O}$	pure water density [kg/m <sup>3</sup> ]
$\rho_{liq}$	liquid product density [kg/m <sup>3</sup> ]
$\rho_{MeOH}$	pure methanol density [kg/m <sup>3</sup> ]
$\rho_{wash}$	washcoat density [kg/m <sup>3</sup> ]
$\omega_{MeOH}$	methanol mass fraction in liquid product [kg/kg]
<b>Superscripts</b>	
<i>in</i>	reactor inlet
<i>out</i>	reactor outlet

Normal conditions are defined at 273 K and 1 bara.

When employed in multi-tubular fixed-bed reactors, structured catalysts having substrates made of highly conductive materials, like e.g. aluminum or copper, exhibit remarkably high radial effective thermal conductivities, which are further enhanced by adopting substrates with relatively low void fractions [8–11]. This plays a key role in determining the reactor performances, especially in terms of heat transfer properties [12,13]: heat exchange does not anymore rely on a convective mechanism, but on a conductive one within the metallic matrix of the structured substrate, which is independent of the gas flow rate in reactor tubes.

These properties make highly conductive structured catalysts promising for the intensification of a number of existing catalytic processes, especially those involving highly exothermic/ endothermic gas/solid and gas/solid/liquid reactions in which large

temperature gradients should be avoided to control selectivity and/or catalyst deactivation [8,14–18]. In particular, thanks to their prevailing conductive heat transfer mechanism which is, contrary to the convective mechanism, independent of the reactor tube length, such catalytic systems can be adopted for the operation of compact reactors, otherwise potentially unfeasible with conventional packings [11].

In a recent paper we showed by simulation that, when applied to the methanol synthesis, highly conductive structured catalysts such as washcoated copper open-cell foams (OF) and honeycomb monoliths (HM), in addition to limited pressure drop and minimal impact of intraporous mass transfer limitations, enable compact multitubular reactors to operate with limited hot-spot and recycle ratios with respect to conventional packings [7]. Such configurations are particularly interesting from the industrial point of view, since they would open new scenarios for the development of small-scale methanol synthesis processes, particularly appealing for the exploitation of feedstock available in limited amounts (e.g. syngas from biomass or stranded/associated natural gas reservoirs).

The preparation of conductive structured catalysts for the methanol synthesis has been scarcely investigated in the literature. The most relevant work dealing with this topic is that of Phan et al. [19] who carried out the methanol synthesis over steel monoliths prepared from corrugated and flat Fecralloy sheets coated with a ball-milled aqueous slurry of Cu/ZnO/Al<sub>2</sub>O<sub>3</sub> catalyst synthesized by a two-stage coprecipitation method. The authors claim that the observed superior activity of the monoliths compared to packed-bed reactor could be related to the thermal properties of the monoliths, i.e. to their ability to keep the catalytic bed nearly isothermal for all the studied CO conversion levels (up to 30%).

In this work we study the preparation of prototype copper open-cell foams, washcoated with a commercial Cu/ZnO/Al<sub>2</sub>O<sub>3</sub> catalyst. We report the results of the chemical testing of our prototypes of conductive structured catalysts in the low temperature-low pressure methanol synthesis at relevant industrial conditions and we compare their performances with those of the original commercial powdered catalyst. Eventually, we also report the results of an additional campaign of activity tests carried out with both the washcoated foams and the original powdered catalyst under RWGS reaction conditions at  $T=505$  K and  $P=1$  bara for comparison purposes.

## 2. Materials and methods

### 2.1. Washcoating

Following standard recipes developed in our laboratories for alumina supported catalysts [20–22], we performed preliminary investigations by adding 150 ml of an aqueous HNO<sub>3</sub> solution 65 wt.% to the commercial powdered catalyst while stirring. Elemental analyses revealed a metal loss in the mother liquors of about 0.075 g<sub>Cu</sub>/g<sub>powder</sub> and 0.083 g<sub>Zn</sub>/g<sub>powder</sub> after ultracentrifugation (Hermle Z323K) at 13 krpm and 298 K for 30 min. This suggested that standard slurry recipes making use of HNO<sub>3</sub> to disperse the powders in the suspension by particles surface charging could not be applied in this case.

Accordingly, following the best recipe proposed by Germani et al. [23], we prepared slurries by ball-milling a mixture containing 100 g of deionized water, 25.25 g of commercial powdered catalyst and 0.7 g of Tylose® MH 300 P2 (Methylhydroxyethylcellulose,  $MW=95,000$  g/mol, [24]) as dispersant. More specifically, we used 3.5 g ZrO<sub>2</sub> spheres/g powder as grinding bodies (about 1 cm as diameter) [21]. We mixed the ingredients in a 250 ml PE sealed jar, which was then kept rotating at 40 rpm overnight. In this regard, it has to be noted that, on following the Germani

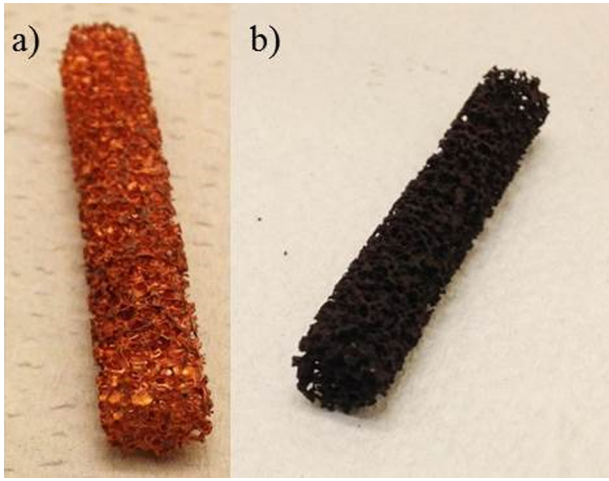


**Fig. 1.** Sample of 45 PPI,  $\varepsilon = 0.936$  open-cell copper foam (a) before coating and (b) after 2 coating layers deposition (14 wt.% washcoat load) and subsequent calcination.

et al.'s actual procedure [23] which includes stirring instead of ball-milling, unstable slurries were obtained. Indeed, too coarse catalyst particles ( $d_{50} = 38 \mu\text{m}$ ) settled after stirring over 24 h. Stable dispersions were instead obtained by ball-milling. Moreover, metal loss in the mother liquors was proved to be negligible in this case (i.e. at least two orders of magnitude lower than that obtained when adopting standard acidic suspensions).

Part of the slurry was dried at 383 K for 24 h and calcined from RT to 573 K, 1 K/min,  $t_{\text{hold}} = 2$  h, as representative sample of the washcoat layer prior to deposition on structured substrate. Such a sample will be named “slurried powders” in the following.

The slurry rheological behavior was analyzed at 293 K by a rotational rheometer (Reologica Instruments Stresstech 500) equipped with a 40 mm flat-plate. Shear rates between 1 and  $100 \text{ s}^{-1}$  were investigated. The granulometry of the original and suspended powders was measured by a laser particle size analyzer (Cilas 1180).

Cylindrical ( $L_{\text{foam}} = 50$  mm,  $d_{\text{foam}} = 8$  mm) samples of copper open-cell foams were cut by electroerosion from samples supplied by Porvair, Inc. (Hendersonville, NC) and used for this work (Fig. 1a). The foams were characterized by pycnometry and optical microscopy (Olympus SZ-CTV), in terms of void fraction, pore diameter, cell diameter and strut diameter (Table 1). Interestingly, these values were found to be reasonably in line with those predicted by Lu et al.'s cubic cell model [25]. From the pore diameter, the foam pore density (PD) was then derived as  $PD = 25.4/a$ , which provided a pore density of 45 PPI.

Due to the fact that copper is readily attacked by acids like  $\text{HNO}_3$ , which causes metal dissolution and bulk oxidation (instead of formation of a self-protective, highly porous, oxide layer) when heated in air [26], we decided not to pre-treat our substrates with thermal or chemical processes to keep copper thermal properties unchanged. Accordingly, bare copper foam samples were only washed with deionized water and acetone to remove dust and other impurities.

**Table 1**  
Geometrical characterization of the tested open-cell foam.

Dimension	Symbol	Measured value
Void fraction	$\varepsilon$	0.936
Pore diameter	$a$	0.564 mm
Cell diameter	$d_c$	1.289 mm
Strut diameter	$d_s$	0.212 mm

Cleaned copper foams were then dipped in the ball-milled slurry and withdrawn at constant speed (3 cm/min). A strong  $\text{N}_2$  flow was then applied to blow the excess slurry out from the 3D network of struts [27]. Drying in static air at RT overnight and calcination in static air from RT to 573 K, 1 K/min as heating ramp followed [19,23]. The temperature was then kept at 573 K for 2 h and later decreased to RT in 1 h. TG-DTA experiments (from RT to 1273 K, 10 K/min,  $\text{N}_2$  atmosphere) pointed out that thermal decomposition of Tylose occurs at about 423–448 K, suggesting that no residues of Tylose remain in the washcoated sample after calcination. Multiple layer deposition technique was adopted to increase the washcoat load, which consisted in repeatedly dipping the substrate in the slurry, blowing the excess slurry out and drying in air at RT before two consecutive dippings. Washcoat load after each coating cycle was evaluated by weight measurements. Washcoat textural properties (i.e. homogeneity, presence of cracks) were evaluated by optical microscopy (Olympus SZ-CTV).

The washcoat volumetric fraction  $\xi$  was evaluated from the washcoat load and the foam volume as:

$$\xi = \frac{V_{\text{wash}}}{V_{\text{foam}}} = \frac{W_{\text{wash}} / \rho_{\text{wash}}}{V_{\text{foam}}} \quad (1)$$

with washcoat density  $\rho_{\text{wash}} = 650 \text{ kg/m}^3$  estimated from preliminary coating investigations on copper slabs.

The washcoat thickness  $\delta_{\text{wash}}$  was therefore calculated from washcoat volumetric fraction and strut diameter, assuming cylindrical struts and uniform coverage:

$$\frac{V_{\text{wash}}}{V_{\text{struts}}} = \frac{\xi}{1 - \varepsilon} = \frac{(d_s + 2\delta_{\text{wash}})^2 - d_s^2}{d_s^2}$$

$$\Rightarrow \delta_{\text{wash}} = \frac{d_s}{2} \times \left( \sqrt{\left(1 + \frac{\xi}{1 - \varepsilon}\right)} - 1 \right) \quad (2)$$

## 2.2. Setup for activity tests

The setup for catalytic activity tests included a stainless steel tubular reactor ( $ID = 9.14$  mm,  $L = 41.3$  cm), equipped with an axial N-type sliding thermocouple and placed inside an electric furnace (Kanthal Fibrothal heating modules, maximum duty: 450W). A second axial N-type thermocouple was inserted in the reactor from the bottom to measure the bottom side of the catalytic bed in the case of the washcoated copper foam tests. Pre-mixed reactant mixture was fed by means of a digital mass flow controller from a high purity aluminum coated gas cylinder.

A pressurized pot for collecting liquid products was placed downstream the reactor and kept refrigerated at 290 K by an external cooling bath. Reactor pressure was regulated by means of a digital back pressure controller. Off-gas were sent to an on-line gas chromatograph (Agilent 6890N) equipped with a Carbosieve column connected to a thermal conductivity detector (TCD). Back-flush for  $\text{CO}_2$  on this channel was operated by means of a Porapak Q column installed before the Carbosieve column. In parallel, a FFAP capillary column was installed and connected to a flame ionization detector (FID) for hydrocarbons and oxygenates quantification. An additional dedicated Porapak Q column was installed on the TCD channel to be used for off-line liquid product analysis by means of manual injection with a microsyringe.

Activity tests were performed on both the commercial powdered catalyst and the washcoated copper foam. Slurried catalyst powders were also tested with the scope of identifying any effect of the slurry preparation step on the catalyst activity.

0.4 g of catalyst powders were loaded into the reactor, diluted 8:1 wt./wt. with high purity 75–150  $\mu\text{m}$  SiC powder to prevent

strong temperature gradients along the catalytic bed. The resulting catalytic bed length was around 3 cm.

For OF tests, two samples of washcoated copper foams (14 wt.% washcoat load, Fig. 1b) were loaded in the reactor in each test, to obtain an active phase loading similar to that of the packed-bed. In this case, the overall catalytic bed height was around 10 cm. Noteworthy, the foams diameter was smaller than the inner reactor tube diameter to facilitate the loading/unloading of the foams at room temperature without damaging the coating layer. In order to avoid catalyst by-pass phenomena due to the clearance between the foam and the reactor wall, each foam was wrapped with quartz-wool tape before being loaded in the reactor. The thermal insulating properties of the tape were not an issue in this case, because the aim of the lab-scale activity testing was not to demonstrate the good heat transfer properties of the metal foam (to be instead verified on a pilot scale reactor), but to check that no significant variations in the catalytic activity of the structured catalyst occurred after the coating procedure.

Two layers of quartz wool a few millimeters thick were eventually placed at the top and bottom of the catalytic bed to keep it in place and to trap the catalyst possibly detaching from the structured substrate during the experiments.

The catalyst was reduced at 1 bara under 200 cm<sup>3</sup>/min N<sub>2</sub>/H<sub>2</sub> (3:1 v./v.) flow at NTP, the furnace temperature being increased from RT to 503 K at 1 K/min. The system was then kept at temperature for 2 h. Afterwards, the back-pressure controller was set at 50 bara and N<sub>2</sub> was fed for building-up pressure before feeding syngas. The temperature was eventually adjusted to the desired value. This point was taken as the time zero for the time on stream value (T.o.S.).

Relevant industrial reactor inlet molar composition (i.e. 8.3% CO, 2.6% CO<sub>2</sub>, 73.2% H<sub>2</sub>, 5.1% CH<sub>4</sub>, N<sub>2</sub> to balance, molar basis.  $M=6.5$ ) and pressure (50 bara) were adopted [7]. The space velocity ( $GHSV$ ) was set to 15,000 NI/h/kg<sub>cat</sub>. Three levels of temperature (485, 505 and 525 K) were investigated.

In all the tested conditions, measured axial temperature profiles across packed-beds always showed small deviations from the average and from the nominal values, limited to  $\pm 1$  K. In the case of structured catalysts, the difference between the measured top and bottom temperatures of the catalytic bed was always less than 1 K. Furthermore, the very high thermal conductivity of the substrate made of highly pure copper ( $\sim 400$  W/m/K) let us reasonably assume negligible axial temperature gradients across the whole catalytic bed.

CO<sub>x</sub> conversion was calculated starting from the inlet CO and CO<sub>2</sub> flows and from off-gas analysis as follows:

$$\text{CO}_x \text{ conversion} = \frac{(F_{\text{CO}}^{\text{in}} - F_{\text{CO}}^{\text{out}}) + (F_{\text{CO}_2}^{\text{in}} - F_{\text{CO}_2}^{\text{out}})}{F_{\text{CO}}^{\text{in}} + F_{\text{CO}_2}^{\text{in}}} \quad (3)$$

Net production of CH<sub>4</sub> was found negligible. Methanol in the off-gas was also identified and quantified.

Water and methanol were the most abundant species in the condensed phase. Negligible amounts of other carbonaceous species were found in that fraction. Liquid phase density analysis (DMA 4500 Density Meter, Anton Paar) was therefore performed on all liquid samples taken during high pressure tests. Roughly 24 h were waited to collect enough liquid product for density analysis. Accordingly, the methanol mass fraction in the condensed phase,  $\omega_{\text{MeOH}}$  was calculated as follows:

$$\omega_{\text{MeOH}} = \frac{\frac{1}{\rho_{\text{liq}}} - \frac{1}{\rho_{\text{H}_2\text{O}}}}{\frac{1}{\rho_{\text{MeOH}}} - \frac{1}{\rho_{\text{H}_2\text{O}}}} \quad (4)$$

Methanol productivity was then calculated as:

$$\text{Prod}_{\text{MeOH}} = \dot{M}_{\text{MeOH}}^{\text{off-gas}} + \frac{M_{\text{MeOH}}^{\text{liq}}}{t_{\text{sampl}}} \quad (5)$$

The typical duration of an experimental run was about two weeks. At the end of the two weeks, the catalyst stability was checked at  $T=505$  K.

The same setup was used for the campaign of low pressure tests;  $P=1$  bara,  $T=505$  K and H<sub>2</sub>-rich and CO-free reactant mixture composition (i.e. 4% CO<sub>2</sub>, 80% H<sub>2</sub>, 3% CH<sub>4</sub>, N<sub>2</sub> to balance, molar basis) were used for the purpose, therefore assuring negligible methanol formation as well as high CO<sub>2</sub> conversions at equilibrium. Operating in large excess of hydrogen further helped in boosting the experimental CO<sub>2</sub> conversions. Same catalyst loads and spatial velocity of high pressure tests were adopted during low pressure tests. Due to the difference in pressure, the actual volumetric gas flow rate in low pressure tests was 50-fold that in high pressure tests. Accordingly, transient periods were much shorter in this second campaign of tests.

For both campaigns, carbon balances were evaluated as

$$C_{\text{balance}} = \frac{(F_{\text{CO}} + F_{\text{CO}_2} + F_{\text{CH}_4})^{\text{in}} - (F_{\text{CO}} + F_{\text{CO}_2} + F_{\text{CH}_4} + F_{\text{MeOH}})^{\text{out}}}{(F_{\text{CO}} + F_{\text{CO}_2} + F_{\text{CH}_4})^{\text{in}}} \quad (6)$$

and always closed with errors between 0 and 5%.

### 3. Results and discussion

#### 3.1. Slurry preparation

Particle size distribution of the dispersed catalyst is strongly affected by the ball-milling process. Upon 24 h of wet milling, a bimodal distribution, with two maxima at 2 and 4  $\mu\text{m}$ , was measured for the suspended powders. It has to be compared with the monomodal particle size distribution, centered at around 38  $\mu\text{m}$ , of the original powder (Fig. 2).

Notably, ball-milled slurries suffered from air bubbles entrapment, likely due to the long-chain polymeric structure of Tylose, acting as “foaming” agent. Air bubbles could not be removed even by ultrasounds.

Nevertheless, slurries rheology was reproducible, showing non-Newtonian shear-thinning behavior, characterized by a viscosity decreasing on increasing the shear rate (Fig. 3). Furthermore, rheological curves were found to be in line with those of typical slurries used in other similar washcoating activities [21,22].

#### 3.2. Slurry deposition

Single layer deposition on copper foams led to a washcoat load around 6–9 wt.%. Optical microscopy images of washcoated foams evidenced homogeneous substrate coverage, with no cracks and negligible pore blocking (Fig. 4b). Despite of the air bubbles entrapment, adhesion was satisfactory after the first dip-blowing step.

The deposition of a second washcoat layer brought an increase of the washcoat load, approaching 9–14 wt.%. Minor cracks were observed, but did not significantly affect the washcoat adhesion (Fig. 4c).

By using Eq. (2), we estimate a washcoat thickness of 75  $\mu\text{m}$  in the case of 14 wt.% washcoat load.

In view of increasing the washcoat load, a third deposition was attempted, but no significant weight increase occurred. Furthermore, the evident presence of cracks seriously compromised the washcoat adhesion in this case (Fig. 4d).



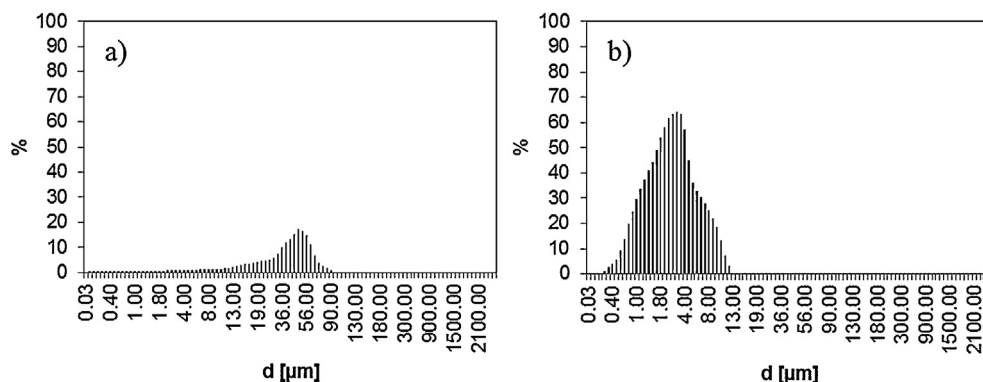


Fig. 2. Particle size distribution before (a) and after (b) slurry ball-milling.

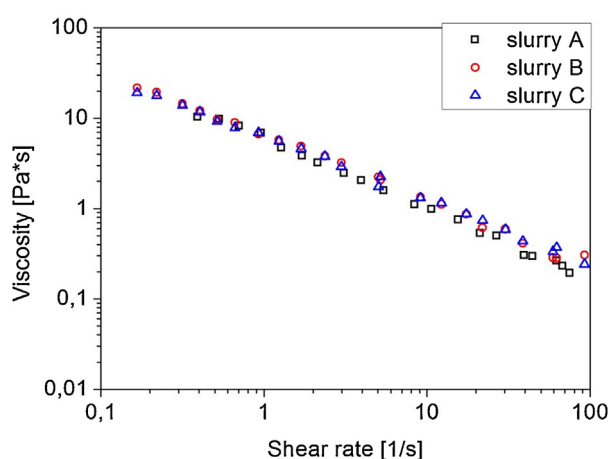


Fig. 3. Rheological behavior of three ball-milled slurries prepared from the same recipe.

For the same purpose, we decreased the velocity of the blowing  $N_2$  flow. However, we observed that, although low  $N_2$  jet velocity easily resulted in thicker washcoat layers, pore blocking was encountered more often. Accordingly, we used a  $N_2$  flow velocity of about 20 m/s.

After calcination, all samples showed washcoat layers resistant to disintegration while handling. Accordingly, foams with 14 wt.% washcoat load were loaded into the reactor. Even after unloading the samples from the reactor, the washcoat loss was limited to less than 20 wt.%, which proved the satisfactory adhesion properties of the so prepared washcoat layers for the purpose of the work. However, in view of future scale-up work, this aspect needs a further optimization study, especially considering the more demanding conditions which the structured catalysts would be subjected to.

### 3.3. Activity tests

#### 3.3.1. High pressure tests

Before testing the structured systems, we verified the chemical inertia of the bare copper foams at the typical methanol synthesis test conditions (blank test). To do this, we loaded the reactor with two uncoated copper foams and, after the same reduction

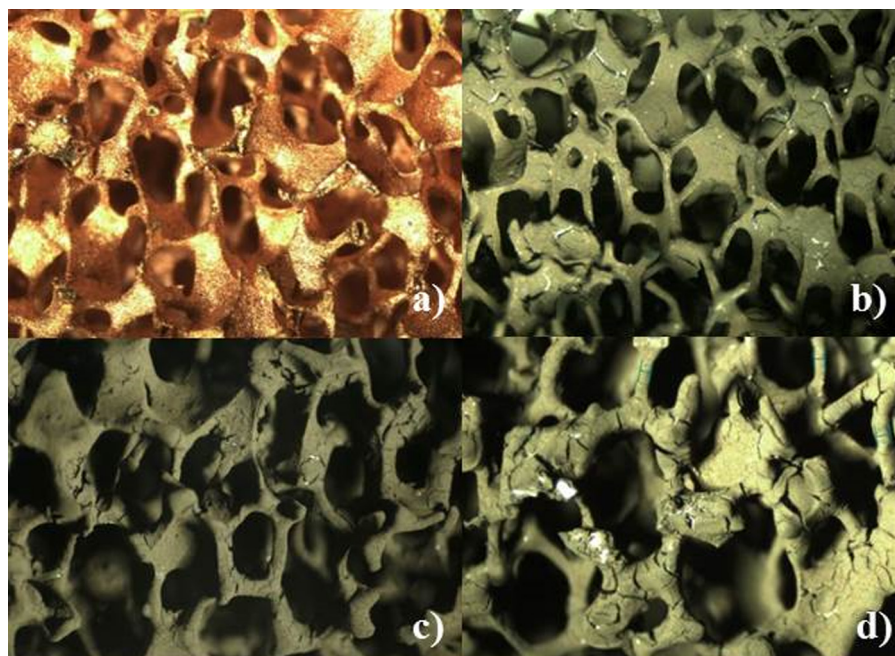


Fig. 4. Optical microscope images of 45 PPI,  $\varepsilon = 0.936$  open-cell copper foam sample (a) bare sample, (b) after 1 coating layer deposition, (c) after 2 coating layers deposition and (d) after 3 coating layers deposition. Samples (b)–(d) were calcined from RT to 573 K,  $t_{\text{hold}} = 2$  h.

treatment adopted for the Cu/ZnO/Al<sub>2</sub>O<sub>3</sub> catalyst, we performed activity tests at the conditions typical of a standard run ( $T=505$  K,  $P=50$  bara, feed composition: 8.3% CO, 2.6% CO<sub>2</sub>, 73.2% H<sub>2</sub>, 5.1% CH<sub>4</sub>, N<sub>2</sub> to balance,  $Q^{in}=100$  cm<sup>3</sup>/min at NTP). The blank test showed absence of any product in the gas phase and zero conversions over about 100 h after the steady-state was reached, therefore confirming the absence of any appreciable catalytic activity of the bare copper substrates.

Performances of the commercial powdered catalyst (CC), slurried powder (SP) and washcoated foam (OF) in terms of CO<sub>x</sub> conversion and MeOH productivity as a function of temperature are compared in Figs. 5 and 6.

As expected, both CO<sub>x</sub> conversion and MeOH productivity increase upon increasing the temperature for all the three investigated catalysts, keeping reasonably far from thermodynamic equilibrium even at the higher investigated temperatures. OF showed however lower CO<sub>x</sub> conversions and MeOH productivities than CC.

In this regard, we exclude the presence of intraporous mass transfer limitations within the washcoat thickness because, from simulation results [7], we expect that such mass transfer limitations should become relevant only for characteristic lengths comparable to those typical of commercial pelletized catalysts (i.e. few millimeters) [28].

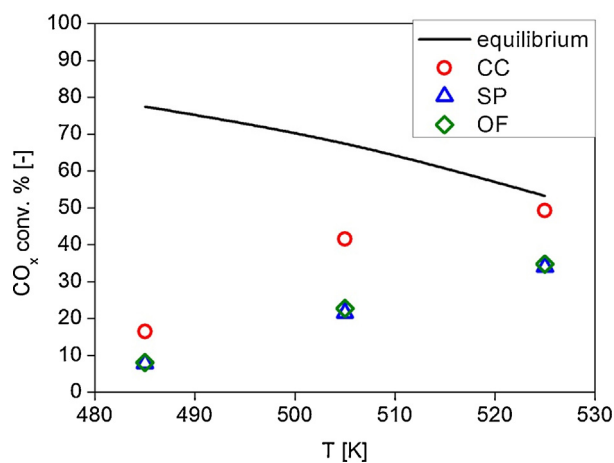


**Fig. 5.** CO<sub>x</sub> conversion over the investigated catalysts (fresh samples) as a function of temperature.  $P=50$  bara,  $GHSV=15,000$  Ni/h/kg<sub>cat</sub>, feed composition: 8.3% CO, 2.6% CO<sub>2</sub>, 73.2% H<sub>2</sub>, 5.1% CH<sub>4</sub>, N<sub>2</sub> to balance.

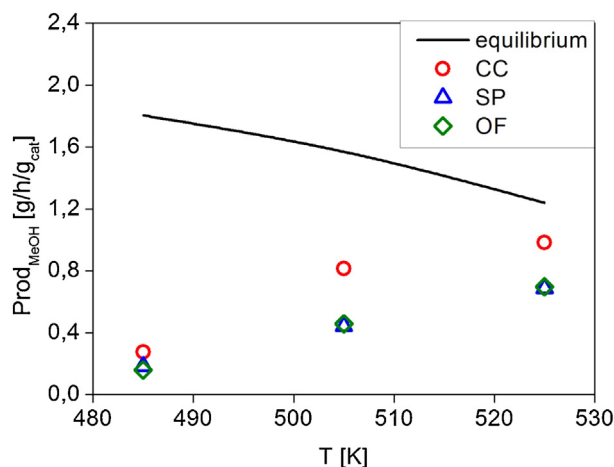


**Fig. 6.** MeOH productivity over the investigated catalysts (fresh samples) as a function of temperature. Same process conditions of Fig. 5.

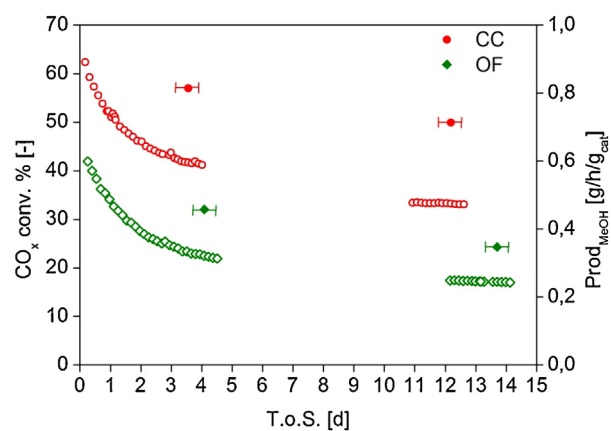


**Fig. 7.** Evolution of CO<sub>x</sub> conversion and MeOH productivity with T.o.S..  $P=50$  bara,  $T=505$  K,  $GHSV=15,000$  Ni/h/kg<sub>cat</sub>, feed composition: 8.3% CO, 2.6% CO<sub>2</sub>, 73.2% H<sub>2</sub>, 5.1% CH<sub>4</sub>, N<sub>2</sub> to balance. Solid symbols: MeOH productivity, empty symbols: CO<sub>x</sub> conversion. The horizontal bar indicates the sampling period.

Interestingly, for all the temperature levels, SP returned very similar activity levels to those of OF, both in terms of CO<sub>x</sub> conversion and MeOH productivity. This evidences that the deposition procedure (i.e. dip-blowing) has not altered the catalyst activity. On the contrary, the slurry preparation and/or calcination procedure seems to be responsible for a change in the catalytic performances. In this regard, it is worth noticing that Echave et al. [29] found a similar result when preparing aqueous slurries of a Pd/ZnO catalyst powder to be washcoated onto Fecralloy corrugated foils. They ascribed the lower activity of the slurried powders to the amphoteric nature of the ZnO (dissolution-re-precipitation process), which caused loss of surface area and consequently lower palladium dispersion. A similar behavior could also have occurred in our catalyst which contained a significant ZnO amount [2], but, unfortunately, due to industrial secrecy restrictions, the commercial catalyst could not be characterized.

In order to verify if the decreased activity of the washcoated samples and of the slurried powders was related to the solvent addition for preparing slurries, preliminary tests were carried out by substituting water with ethanol. Unfortunately, no encouraging results were found. Indeed, coatings prepared from ethanol-based slurries showed similar catalytic activity to those prepared using water. Furthermore, being methylhydroxyethylcellulose less soluble in ethanol than in water, some issues arose when trying to assure both good rheological properties and comparable coating performances. We therefore decided to discard this option.

After two weeks on stream, both CO<sub>x</sub> conversion and MeOH productivity measured with CC decreased of about 20% of their initial steady-state values (taken after four days on stream) (Fig. 7). In line with the literature, we speculate that this effect may be ascribed to copper crystallites sintering [5,30–32]. Interestingly, OF showed a deactivation trend similar to CC, singling out that neither the slurry preparation nor the calcination procedure affects the catalyst stability.

### 3.3.2. Low pressure tests

It is worth noticing that the need of operating at high pressure makes methanol synthesis catalytic tests at relevant industrial conditions highly demanding. From this point of view it would be interesting to identify more convenient but still representative operating conditions for a rapid screening of the intrinsic activity of Cu/ZnO/Al<sub>2</sub>O<sub>3</sub> methanol catalysts.

WGS/RWGS reactions are well-recognized as key reactions taking place in the methanol synthesis process over Cu/ZnO/Al<sub>2</sub>O<sub>3</sub> catalysts, providing an interchange route between CO and CO<sub>2</sub> and

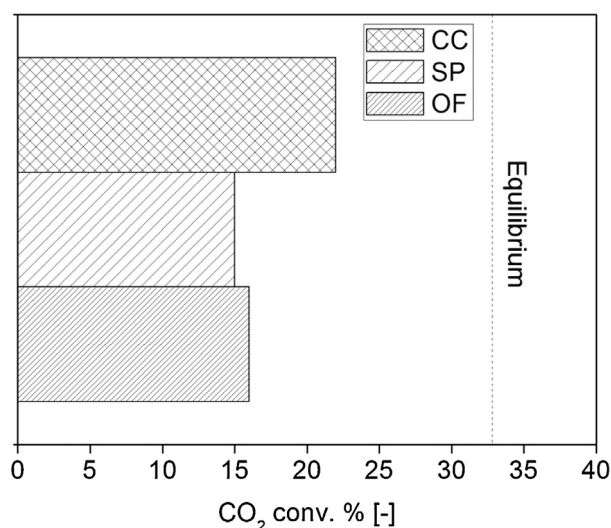


Fig. 8. CO<sub>2</sub> conversion over the investigated catalysts.  $P=1$  bara,  $T=505$  K,  $GHSV=15,000$  Ni/h/kg<sub>cat</sub>.

pushing the methanol synthesis reactions from CO and CO<sub>2</sub> toward the products through water consumption in the WGS step [33,34].

To verify this, we decided to perform an additional campaign of tests with the same experimental apparatus, but using a CO-free reactant mixture composition with H<sub>2</sub>/CO<sub>2</sub> = 20 to test the RWGS reaction at atmospheric pressure. The same three catalytic systems, namely CC, SP and OF, were tested.

As shown in Fig. 8, all the three catalytic systems provided CO<sub>2</sub> conversion levels far from equilibrium, with OF exhibiting lower values than CC. SP, instead, exhibited similar values to OF, thereby confirming that the RWGS activity of the catalyst is also affected by the slurry preparation and/or calcination procedure.

Interestingly, the results collected at low pressure are qualitatively in line with those found in the previous campaign of tests at high pressure in terms of CO<sub>x</sub> conversion and MeOH productivity (Figs. 5 and 6). Similar trends were also found in additional tests performed in a different setup. Accordingly, the analogy between the two sets of data (i.e. high and low pressure tests) suggests that the RWGS reaction can be a representative probe reaction for studying the chemical activity of Cu/ZnO/Al<sub>2</sub>O<sub>3</sub> methanol catalysts, without requiring to operate at the high pressures and with the long transients typical of commercial methanol synthesis process.

#### 4. Conclusions

Washcoating of highly conductive copper open-cell foams ( $PD=45$  PPI,  $\varepsilon=0.936$ ) was successfully carried out by using the slurry method and adopting an aqueous suspension of commercial Cu/ZnO/Al<sub>2</sub>O<sub>3</sub> powdered catalyst, deionized water and methylhydroxyethylcellulose. Single- or multiple-step dip-blowing method was adopted. Washcoat loads up to 9 wt.% were obtained with single-step dip-blowing, while the loading increased to 14 wt.% after two consecutive dip-blowing steps. In both cases, washcoat layers were found to be homogeneous, up to 75  $\mu$ m thickness, with negligible cracks and pore blocking. Washcoated foams were also resistant to disintegration while handling. This was not the case of samples coated with higher catalyst loadings, obtained either by increasing the number of dip-blowings or by reducing the blowing strength.

Washcoated copper foams (14 wt.% washcoat load) were then tested in the methanol synthesis at relevant industrial conditions. They were found to be active in catalyzing the methanol synthesis reaction. This result, together with our previous findings [7,35],

paves the way for the development of a novel compact multitubular reactor for the methanol synthesis loaded with conductive structured catalysts.

The activity of structured catalysts is however lower than that of the original powdered catalyst. Chemical testing of slurried powders pointed out that the slurry deposition step does not affect the final catalytic activity of the structured system. Instead, the slurry preparation and/or calcination step is responsible for a change in the catalytic performances. Preliminary tests were carried out substituting water with ethanol, but no significant differences in the chemical activity were found. Further investigations on this aspect are currently ongoing in our labs.

These results were confirmed by running RWGS experiments at atmospheric pressure. The qualitative accordance between CO<sub>x</sub> conversion/MeOH productivity values collected during high pressure tests and CO<sub>2</sub> conversion values collected during low pressure tests suggests that the RWGS reaction can be considered as a representative probe reaction for ranking the intrinsic activity of Cu/ZnO/Al<sub>2</sub>O<sub>3</sub> methanol catalysts without requiring operation under the high pressures and with the long transients typical of the commercial methanol synthesis process.

#### Acknowledgments

The authors from Politecnico di Milano gratefully acknowledge funding from Total Refining & Chemicals, France, and from the Italian Ministry of Education, University and Research, Rome (MIUR, Progetti di Ricerca Scientifica di Rilevante Interesse Nazionale, prot. 2010XFT2BB) within the project IFOAMS ("Intensification of Catalytic Processes for Clean Energy, Low-Emission Transport and Sustainable Chemistry using Open-Cell Foams as Novel Advanced Structured Materials").

#### References

- [1] G.A. Olah, A. Goepfert, G.K. Surya Prakash, *Beyond Oil and Gas: The Methanol Economy*, first ed., Wiley-VCH Verlag GmbH & Co. KGaA, Weinheim, 2006.
- [2] E. Fiedler, G. Grossmann, D.B. Kersebohm, G. Weiss, C. Witte, *Ullmann's Encyclopedia of Industrial Chemistry*, Wiley-VCH GmbH, Weinheim, 2003, pp. 611.
- [3] K. Klier, V. Chatikavanij, R.G. Herman, G.W. Simmons, *J. Catal.* 74 (1982) 343–360.
- [4] D. Johnson, *Global Methanol Market Review*, 2012, <http://www.ptq.pemex.com/productosyservicios/eventosdescargas/Documents/Foro%20PEMEX%20Petroqu%C3%ADmica/2012/PEMEX.DJohnson.pdf>, Last access: February 17, 2014.
- [5] P.L. Spath, D.C. Dayton, *Preliminary Screening - Technical and Economic Assessment of Synthesis Gas to Fuels and Chemicals with Emphasis on the Potential for Biomass-Derived Syngas*, National Renewable Energy Laboratory, 2003.
- [6] M. Santiago, K. Barbera, C. Ferreira, D. Curulla-Ferré, P. Kolb, J. Pérez-Ramírez, *Catal. Commun.* 21 (2012) 63–67.
- [7] A. Montebelli, C.G. Visconti, G. Groppi, E. Tronconi, C. Ferreira, S. Kohler, *Catal. Today* 215 (2013) 176–185.
- [8] G. Groppi, E. Tronconi, *Chem. Eng. Sci.* 55 (2000) 2161–2171.
- [9] C.G. Visconti, G. Groppi, E. Tronconi, *Chem. Eng. J.* 223 (2013) 224–230.
- [10] E. Bianchi, T. Heidig, C.G. Visconti, G. Groppi, H. Freund, E. Tronconi, *J. Chem. Eng.* 198–199 (2012) 512–528.
- [11] E. Bianchi, T. Heidig, C.G. Visconti, G. Groppi, H. Freund, E. Tronconi, *Catal. Today* 216 (2013) 121–134.
- [12] G. Groppi, E. Tronconi, *Catal. Today* 105 (2005) 297–304.
- [13] A. Shamsi, J.J. Spivey, *Ind. Eng. Chem. Res.* 44 (2005) 7298–7305.
- [14] G. Groppi, E. Tronconi, *Catal. Today* 69 (2001) 63–73.
- [15] G. Groppi, E. Tronconi, C. Cortelli, R. Leanza, *Ind. Eng. Chem. Res.* 51 (2012) 7590–7596.
- [16] O.Y. Podyacheva, A.A. Ketov, Z.R. Ismagilov, V.A. Ushakov, A. Bos, H.J. Veringa, *React. Kinet. Catal. Lett.* 60 (1997) 243–250.
- [17] A.N. Pestryakov, V.V. Lunin, A.N. Devochkin, L.A. Petrov, N.E. Bogdanchikova, V.P. Petranovskii, *Appl. Catal., A: Gen.* 227 (2002) 125–130.
- [18] E. Tronconi, G. Groppi, T. Boger, A. Heibel, *Chem. Eng. Sci.* 59 (2004) 4941–4949.
- [19] X.K. Phan, H. Bakhtiary-Davijany, R. Myrstad, P. Pfeifer, H.J. Venvik, A. Holmen, *Appl. Catal., A: Gen.* 405 (2011) 1–7.
- [20] M. Valentini, G. Groppi, C. Cristiani, M. Levi, E. Tronconi, P. Forzatti, *Catal. Today* 69 (2001) 307–314.
- [21] C. Cristiani, C.G. Visconti, E. Finocchio, P.G. Stampino, P. Forzatti, *Catal. Today* 147 (2009) S24–S29.

- [22] C.G. Visconti, E. Tronconi, L. Lietti, G. Groppi, P. Forzatti, C. Cristiani, R. Zennaro, S. Rossini, *Appl. Catal., A: Gen.* 370 (2009) 93–101.
- [23] G. Germani, A. Stefanescu, Y. Schuurman, A.C. van Veen, *Chem. Eng. Sci.* 62 (2007) 5084–5091.
- [24] SE Tylose GmbH & Co KG, Tylose® MH 300 P2 Technical Data Sheet, SE Tylose GmbH & Co KG, 2005, ([http://setylose.eu/z.tds/TDS\\_e/TDS\\_MH%20300%20P2.B.e.pdf](http://setylose.eu/z.tds/TDS_e/TDS_MH%20300%20P2.B.e.pdf)) (last access: September 25, 2013).
- [25] T.J. Lu, H.A. Stone, M.F. Ashby, *Acta Mater.* 46 (1998) 3619–3635.
- [26] Y.Z. Hu, R. Sharangpani, S.P. Tay, *J. Electrochem. Soc.* 148 (2001) g669–g675.
- [27] A. Montebelli, C.G. Visconti, G. Groppi, E. Tronconi, C. Ferreira, S. Kohler, *Catal. Sci. Technol.* (2014), <http://dx.doi.org/10.1039/C1034CY00179F>.
- [28] G.H. Graaf, H. Scholtens, E.J. Stamhuis, A.A.C.M. Beenackers, *Chem. Eng. Sci.* 45 (1990) 773–783.
- [29] F.J. Echave, O. Sanz, M. Montes, *Appl. Catal., A: Gen.* 474 (2014) 159–167.
- [30] G.C. Chinchén, P.J. Denny, J.R. Jennings, M.S. Spencer, K.C. Waugh, *Appl. Catal.* 36 (1988) 1–65.
- [31] H.H. Kung, *Catal. Today* 11 (1992) 443–453.
- [32] J.T. Sun, I.S. Metcalfe, M. Sahibzada, *Ind. Eng. Chem. Res.* 38 (1999) 3868–3872.
- [33] M.S. Spencer, *Top. Catal.* 8 (1999) 259–266.
- [34] Y. Zhang, Q. Sun, J. Deng, D. Wu, S. Chen, *Appl. Catal., A: Gen.* 158 (1997) 105–120.
- [35] A. Montebelli, C.G. Visconti, G. Groppi, E. Tronconi, C. Ferreira, S. Kohler, *Chem. Eng. J.* (2014) (submitted).